



Contents lists available at ScienceDirect

International Journal of Rock Mechanics and Mining Sciences

journal homepage: <http://www.elsevier.com/locate/ijrmms>

Technical Note

# The significance of displacement control mode in direct shear tests of rock joints

Doron Morad<sup>a,b</sup>, Amir Sagy<sup>b</sup>, Yossef H. Hatzor<sup>a,\*</sup><sup>a</sup> Dept. of Geological and Environmental Sciences, Ben-Gurion University of the Negev, Beer – Sheva, 84105, Israel<sup>b</sup> Geological Survey of Israel, Yehsha'yahu Leibowitz 32, Jerusalem, 9692100, Israel

## ARTICLE INFO

**Keywords:**  
 Rock joints  
 Direct shear  
 Roughness  
 Stick-slips  
 Servo-control  
 Shear strength

## ABSTRACT

Servo-controlled direct shear tests of rough (RMS = 500 μm) and smooth (RMS = 7 μm) surfaces of Gabbro are performed under a constant normal stress of 5 MPa and a constant shear displacement rate of 0.01 mm/s. The tested interfaces are 10 cm long and 8 cm wide. Two servo-controlled shear displacement modes are studied: 1) Piston Displacement Control [PDC], and 2) Block Displacement Control [BDC]. In PDC mode the displacement output from the shear piston is used as the feedback signal for servo control whereas in BDC mode the displacement output from two horizontally oriented LVDT's positioned directly on the sheared interface are used for control. We find that when the surfaces are tested under BDC mode they exhibit a distinct peak shear stress followed by a stress drop to residual shear strength, whereas a continuous transition to "steady state" sliding is exhibited by the same surfaces when tested under PDC mode. This leads to the important observation that while peak shear strength is similar in both control modes the residual shear strength in PDC mode is distinctly higher. All tested interfaces exhibit stick-slip oscillations, the magnitude and frequency of which are strongly related to the control mode. We show that stick slip amplitude and frequency are artificially higher in BDC mode because of servo-control effects and that the correct stick slip behaviour can only be obtained in PDC mode. We find that the displacement control mode in direct shear tests drastically affects the obtained results and therefore investigators must consider the consequences before specifying which servo-control mode to use in direct shear tests.

## 1. Introduction

Direct shear experiments for rock joints are typically conducted under a controlled shear displacement rate and a fixed normal stress. The ISRM suggested method for example<sup>1</sup> prescribes two consecutive test segments: 1) a normal load segment, during which normal stress is applied to the desired level under a constant normal load rate, and 2) a shear load segment, during which the interface is sheared at a controlled shear rate while the target normal stress is maintained at a constant level throughout the shear segment. The issue of the precise location of the shear displacement feedback signal in the testing apparatus is seldom discussed. In experimental civil engineering studies concerning slope stability and underground excavations the shear displacement feedback signal often comes from the motion of the sheared interface since such studies typically consider motion of particular bodies across a plane of discontinuity in the rock mass.<sup>2–4</sup> In seismological applications however, where the motivation is to simulate earthquake mechanics in the lab, the feedback signal for shear displacement may come from the motion of

the loading piston which is located at some distance from the tested interface (see Ref. 5–10), as such studies are primarily concerned with the shear response of geological faults to the application of far field stresses stemming from the interactions across tectonic plate boundaries.

In this technical note we define and distinguish between two shear displacement control modes: 1) Piston Displacement Control (PDC), and 2) Block Displacement Control (BDC), both of which are appropriate for direct shear testing of rock interfaces, depending on the application. We argue that PDC mode represents far field loading of a sheared interface, as would be the case for example in geological faults and large catastrophic landslides. In such cases the stiffness of the rock mass between the loading point and the sliding interface is mobilized during the deformation and affects the shear failure process. In contrast, the BDC mode represents the displacement of a single block across a sheared interface in the field, where the stiffness of the rock mass between the loading point and the sliding block is irrelevant as the load on the block is mainly derived from body forces or forces transmitted from boundary

\* Corresponding author.

E-mail address: [hatzor@bgu.ac.il](mailto:hatzor@bgu.ac.il) (Y.H. Hatzor).<https://doi.org/10.1016/j.ijrmms.2020.104444>

Received 12 March 2020; Received in revised form 14 June 2020; Accepted 15 July 2020

Available online 15 August 2020

1365-1609/© 2020 Elsevier Ltd. All rights reserved.

blocks. We show in this paper that the two control modes yield different results and therefore the applied control mode should be considered in light of the application in the field before direct shear tests are conducted in the lab.

In the PDC mode the rate of displacement of the shear piston is controlled using an accurate displacement transducer located inside the actuator ram, while monitoring the displacement of the tested interface. In the BDC mode the rate of displacement of the interface is controlled using accurate displacement transducers that are mounted very close to the tested interface. The main difference between the two control modes is the involvement of the shear machine stiffness in the studied shear deformation process. Typically in direct shear load frames the piston that delivers the shear force, sometimes referred to as the “loading point”, is connected to a steel arm that in turn is connected to the shear frame which hosts the shear box in which the interface is cast in cement. Although each of these elements has its own stiffness, this complex configuration may be simplified to a loading point acting on a single spring with stiffness  $k_m$ , which is connected to a mass  $m$ .

The machine stiffness ( $k_m$ ) is usually a constant number, representing a summation of several structural and material components connected in series between the piston and the sample. Ideally it would be designed to be as stiff as possible so as to minimize machine stiffness effects. The interface stiffness  $K_i$  however may vary quite significantly between samples as it depends on the level of normal stress, the surface roughness, and the shear displacement rate.<sup>11–14</sup> When the machine stiffness is equal to or higher than the interface stiffness ( $k_m \geq k_i$ ) stable sliding will be obtained after ultimate frictional resistance is reached, and the idealized spring and the mass will move in harmony. When the machine stiffness is lower than the interface stiffness however ( $k_m < k_i$ ), instabilities, typically in the form of stick slip oscillations, may ensue at the post peak region. The most fundamental work on stick slip oscillations was done by Rabinowicz<sup>15</sup> who has introduced the “spring-rider” model to explain stick slip oscillations. Rabinowicz suggested that the transition from a higher static ( $\mu_s$ ) to a lower dynamic ( $\mu_d$ ) friction coefficient is the main reason for stick slip oscillations, provided that the machine stiffness and the rider velocity are sufficiently low; indeed he showed that stick slip amplitude may drop to zero if the machine stiffness is high enough and/or the rider velocity is high enough.

The issue of sliding instability has been researched extensively in the past several decades mainly in the context of seismology, following the observations of Brace and Byerlee<sup>16</sup> and Byerlee and Brace<sup>17</sup> of stick slips in the post peak region of triaxial tests, leading to the definition of the important concepts of the critical slip distance  $d_c$ <sup>5</sup> and critical interface stiffness  $k_{crit}$ <sup>18</sup>. Ruina,<sup>10</sup> showed that the critical interface stiffness is given by:

$$k_{crit} = \frac{\sigma_n(B - A)}{d_c} \quad (1)$$

where  $B$ ,  $A$  and  $d_c$  are Dieterich's rate and state friction parameters and  $\sigma_n$  is the normal stress.

A complete analytical solution for the problem of stick slip oscillations in the context of the original spring rider model is presented by Jaeger, Cook and Zimmerman<sup>19</sup> who assume that the static friction coefficient ( $\mu_s$ ) is greater than the dynamic friction coefficient ( $\mu_d$ ), and that the value of the dynamic friction coefficient remains constant throughout the cycles, namely no velocity weakening during stick slip events. Two important results are obtained from the analytical solution of the ideal spring – rider model:

1. The value of the dynamic friction coefficient ( $\mu_d$ ) is given by the mean of the maximum ( $\mu'$ ) and minimum ( $\mu$ ) friction coefficient per stick slip cycle:

$$\mu_d = \frac{\mu' + \mu}{2} \quad (2)$$

2. The displacement per stick slip event  $\Delta x$  is determined by the force drop during a stick slip event, and the stiffness of the spring  $k$ :

$$\Delta x = (T_{max} - T_{min})/k \quad (3)$$

In this technical note we explore two different loading configurations, PDC vs. BDC, and compare the results. In the PDC mode we control the rate of displacement of the shear piston while monitoring the response of the block, a boundary condition identical to the conventional spring – rider model. In the BDC mode we control the rate of displacement of the block while monitoring the piston displacement, a boundary condition that is more standard in rock mechanics and geotechnical engineering applications. We show that the control mode has a dramatic effect on the resulting shear stress – shear displacement behaviour and discuss plausible explanations to the different behaviours.

## 2. Methods

We perform direct shear tests under constant normal stress of 5 MPa and controlled shear displacement rate of 0.01 mm/s using the hydraulic, closed-loop servo-controlled TerraTek direct shear system at Ben-Gurion University rock mechanics laboratory (see Fig. 1, right panel). The normal force capacity is 1000 kN and the shear force capacity is 300 kN. Both the normal and shear piston can be operated under either load or displacement control, thus allowing great flexibility in determining the test boundary conditions. Samples for direct shear testing are prepared by four – point bending of Gabbro prisms, the fractured surface of which is then ground to the desired roughness level (see Fig. 1 – left panel).

The shear system assembly is comprised of three main components (see Fig. 2): 1) horizontal piston; 2) two steel arms, the lower one connected to the shear piston and the upper one is fixed; 3) upper and lower shear boxes. The position of the piston, sometimes referred to as “load point position”, is servo-controlled using output from a magnetic transducer labelled  $S_y$  in Fig. 2 with 0.5% linearity full scale. The horizontal stroke of the piston is 100 mm with 0.5% linearity full scale. Shear displacement between the two blocks is monitored using two LVDT's (labelled  $Y_a$  and  $Y_b$ ) that are mounted on both sides of the tested interface, each with a maximum range of 50 mm and 0.25% linearity full scale. The lower shear box is connected to the lower piston arm whereas the upper shear box is fixed against horizontal motions. When a constant normal stress boundary condition is used, the upper shear box is free to move in the vertical direction, the motion of which is monitored by four vertical LVDT's (labelled  $X_a - X_d$ ) mounted on four corners of the shear box, each also with 50 mm range and 0.25% linearity full scale.

The samples are cast in steel templates that are then positioned in the shear boxes. The maximum allowable specimen width, length, and height is 150 mm X 150 mm X 230 mm. The total length of the shear frame assembly is 1320.8 mm and the total height is 508 mm. The steel arm that connects between the piston and the shear box is 650 mm long. Naturally the effective stiffness of the shear system is affected not only by the materials and lengths of the components, but also by the compressibility of the oil in the shear actuator, O rings, different nuts and bolts, etc. In order to facilitate the discussion, we can represent the effective stiffness of the shear system by a spring stiffness  $k_m$  as schematically illustrated in Fig. 3.

As explained in the introduction, we distinguish between piston displacement control (PDC) and block displacement control (BDC) modes. In PDC mode the piston is moved at a constant velocity and the system stores elastic strain energy during the loading segment according to the applied shear force in the system and the machine stiffness  $k_m$ . In case of instability at the post peak region in the form of a stick slip event a spontaneous force drop will take place followed by spontaneous acceleration of the block. The horizontal distance travelled by the block during this single slip event will be controlled by  $k_m$  and the force drop,

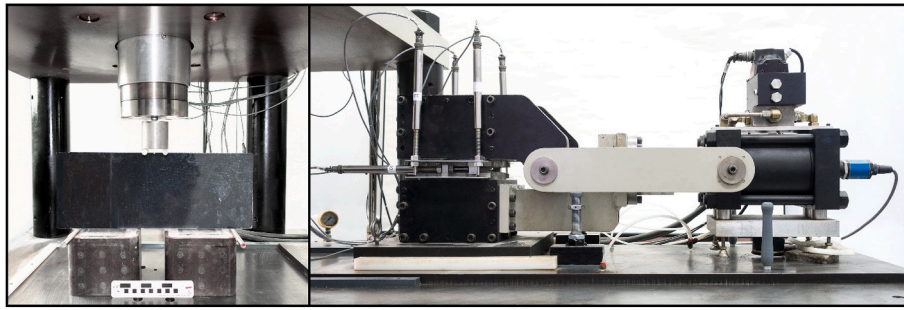


Fig. 1. The direct shear system showing the shear piston, shear box and displacement transducers (right panel), and the normal load frame when used for tensile splitting of a gabbro beam (left panel).

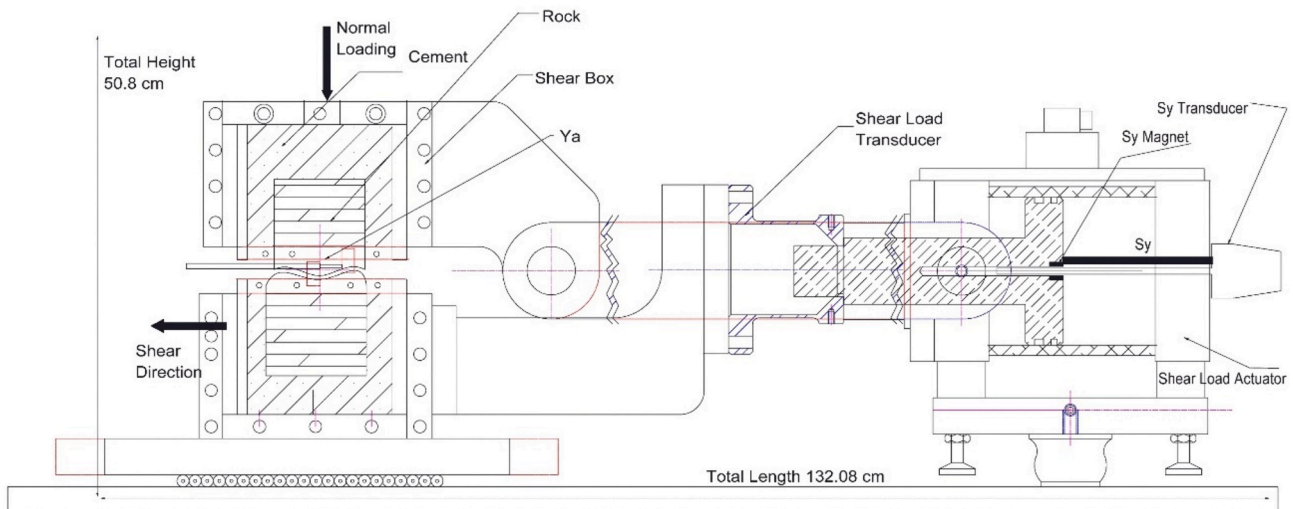


Fig. 2. Technical diagram of the shear system assembly.

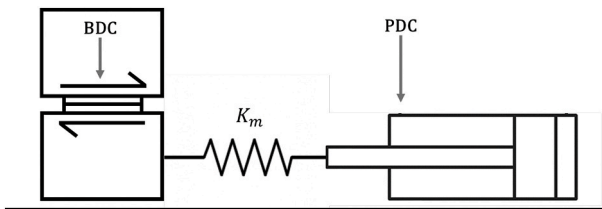


Fig. 3. Schematic illustration of the Piston Displacement Control (PDC) and Block Displacement Control (BDC) modes.  $k_m$  represents the effective stiffness of the shear system.

as per Eq. (3) above. Because the piston and not the block motion is controlled, the system will not try to correct for this spontaneous forward jump, and forward motion of the piston at the prescribed rate will not be interrupted. This is not the case in BDC mode. At the instant of stick slip instability, the forward acceleration of the block will violate the prescribed displacement rate of the block, and therefore the servo-control system will command the piston to retract backwards to correct back to the prescribed block displacement rate.

The machine stiffness  $K_m$  can be determined as the absolute contraction of the spring for a given shear force.<sup>20</sup> A good estimate of the shear load frame stiffness can be obtained during a linear shear loading segment from the force applied in the horizontal direction ( $\Delta F_y$ ) and the difference between the absolute piston motion ( $S_y$ ) and the block motion ( $Y_{av} = \frac{Y_a + Y_b}{2}$ ):

$$k_m = \frac{\Delta F_y}{(S_y - Y_{av})} \quad (4)$$

We consider the effective machine stiffness measurements of the sawcut samples more reliable because rough asperities formed in the fractured beams tend to prompt nonlinear response to shear load and therefore may obscure the machine stiffness calculations.

When running a test the effective machine stiffness during reloading segment as obtained from Eq. (4) should be very close to the value obtained when analysing force drop and displacement during spontaneous stick slip events as per Eq. (3) ( $k_m = \frac{\Delta F_y}{\Delta Y_{av}}$ ). This is demonstrated in Fig. 4, where the piston displacement ( $S_y$ ), the block displacement ( $Y_{av}$ ), and the effective machine displacement ( $S_y - Y_{av}$ ) are plotted vs. shear load during a reloading segment following a spontaneous stress drop after stick slip has occurred. The effective machine stiffness thus obtained is  $k_{m(measured)} = 99523 \text{ N/mm}$ . By calculating those slopes for several reloading segments, we derived statistically a machine stiffness of  $94953 \text{ N/mm}$  with a standard deviation of  $5978 \text{ N/mm}$ .

In Fig. 5 we present a compilation of all the force drops and horizontal slip distances measured in test Gb\_22 which was performed in PDC mode, between 4 and 8.5 mm of block displacement. The slope of this curve returns a calculated machine stiffness of  $k_m = 96,193 \text{ N/mm}$  with a regression coefficient of  $R^2 = 0.98$ . The effective machine stiffness measured in the post peak region during reloading segments and instantaneous unloading segments of stick slip instabilities are presented in Fig. 6. The agreement between the measured machine stiffness from the system response (Eq. (4)) and the calculated machine stiffness as obtained from the analytical solution for stick slips when loading is

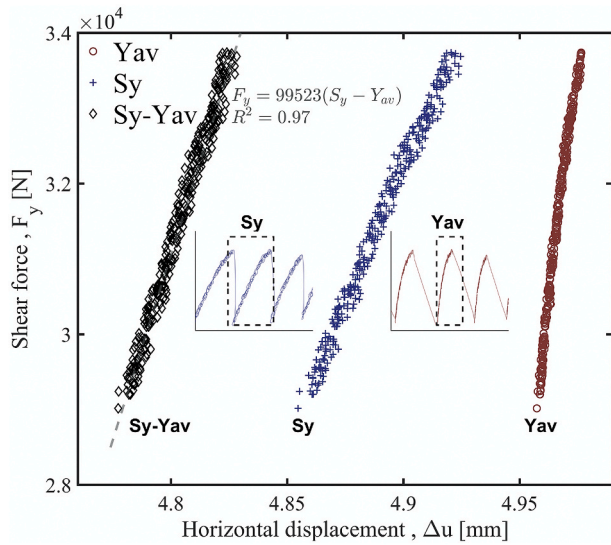


Fig. 4. Piston displacement ( $S_y$ ), block displacement ( $Y_{av}$ ), and the effective machine displacement ( $S_y - Y_{av}$ ) vs. shear load during a typical reloading segment following a stick slip event (test Gb-22).

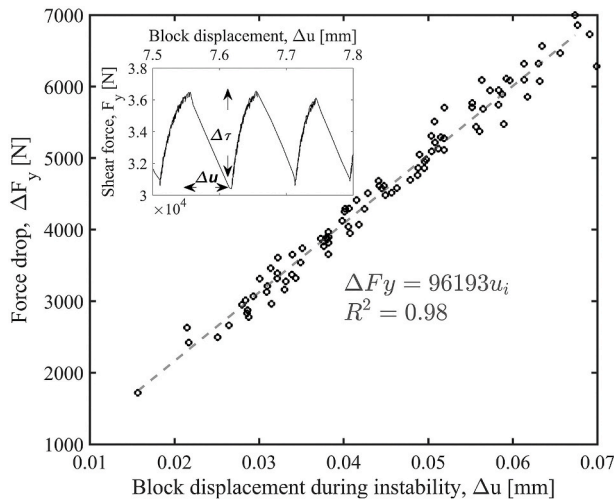


Fig. 5. Force drop  $\Delta F_y$  vs. slip distance during spontaneous slip events when loading is performed in PDC mode. The obtained slope is in very good agreement with the measured machine stiffness value  $K_m$  of 94953 N/mm.

conducted in PDC mode (Eq. (3)) is quite striking, with a difference between methods not exceeding 1.3%.

The starting material for all direct shear tests is Gabbro which can be obtained commercially from the Shanxi Black Granite Quarry in China,

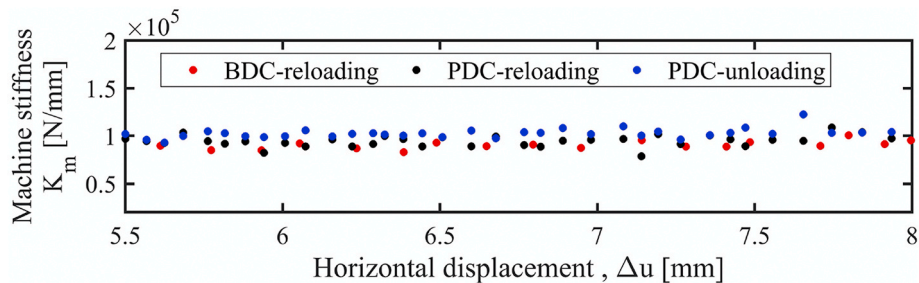


Fig. 6. Machine stiffness measurements calculated using Eq. (3) during instantaneous unloading following stick slip instabilities (applicable only for PDC mode) and during reloading using Eq. (4). The measurements were obtained after peak shear resistance, between 5.5 and 8 mm displacement.

characterized by average grain size of 0.4 mm and bulk density of  $3.05 \frac{g}{cm^3}$ . Static Young's modulus and Poisson's ratio of the intact rock material were obtained by uniaxial compression of a 54 mm diameter solid cylinder tested under a constant strain rate of  $10^{-6} s^{-1}$  in the TerraTek triaxial system at BGU Rock Mechanics Laboratory. The Young's modulus and Poisson's ratio thus obtained are 97 GPa and  $0.19 \pm 0.02$ , respectively. Acoustic velocities of the intact material were tested at BGU with Vinci's AVS system and the obtained dynamic Young's modulus and Poisson's ratio are 119 GPa and 0.24, respectively.

The initial roughness profiles of the sheared surfaces were measured using a laser profilometer model type Conoscan-10 manufactured by Optimet. Two levels of roughness are studied here. The coarser roughness profile was obtained by four-point bending of a solid Gabbro prism (see Fig. 1) with the obtained fractured roughness profile unaltered (for procedure see 21, 14). The characteristic roughness RMS for this sample is more than 500  $\mu m$  and the test began in fully mating initial configuration. The smoother surface was obtained by saw-cutting a Gabbro prism, thus obtaining characteristic RMS of 7  $\mu m$ . Each pair of interfaces (RMS = 500  $\mu m$  and RMS = 7  $\mu m$ ) was analysed spectrally and the results portray very similar statistical roughness values for a given length (see Fig. 7). It can be inferred from Fig. 7 that the smooth interface reaches roughness saturation at 10 mm length whereas the rough interface is characterized by increasing asperity amplitude with increasing measurement length throughout the available sampling length. The average interface size is 10 cm length and 8 cm width, with the lower interface length typically fixed at 12 cm to ensure proper contact between the

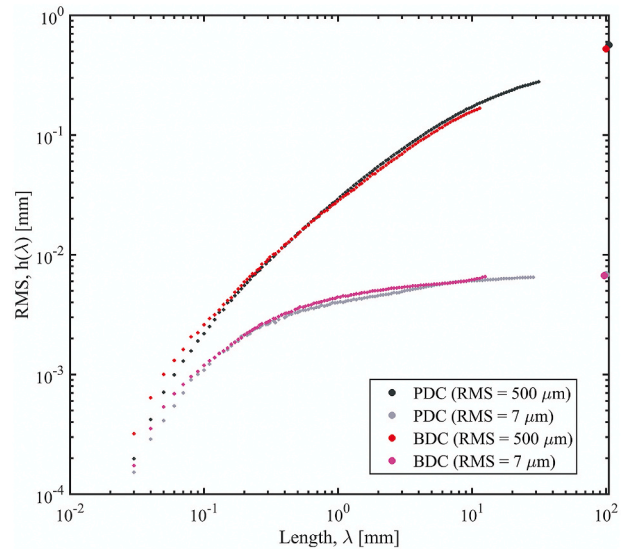


Fig. 7. RMS roughness of initial tested surfaces. Any single trend represents RMS calculations of hundreds of profiles. Complete sample description can be found in Table 1.

upper and lower blocks throughout the shearing segments, to minimize end effects.

The experimental procedure begins with lowering the normal piston at constant stress rate of 0.01 MPa/s until the 5 MPa target normal stress is reached while the interface is held in a fixed position. Afterwards, the shear piston is activated with a constant displacement rate that is usually fixed at 0.01 mm/s. As explained above, the shear displacement rate is controlled either through output from the shear piston position ( $S_y$ ), namely PDC mode, or through output from the pair of horizontal LVDT's mounted close to the interface ( $Y_{av}$ ), namely BDC mode. In each test the relative displacement target between the upper and the lower interface is set to 8.5 mm. Data acquisition rate in all tests is set to 50 Hz (50 counts per sec.) in all displacement and load channels.

### 3. Results

#### 3.1. Direct shear tests

All four direct shear tests were performed under the same normal stress level and under the same shear rate so that the influence of surface roughness on the results can also be discerned. Initial RMS values for the four surface types are shown in Table 1. Shear stress vs. shear displacement curves obtained for both surface types under BDC and PDC modes and shown in Fig. 8 in red and grey shades, respectively. It can be clearly seen that the BDC mode exhibits a distinct peak shear stress region followed by a stress drop to residual shear strength. In contrast, the results obtained under PDC mode do not exhibit a pronounced peak shear stress; rather, a gradual transition to “steady state” sliding is observed, with no significant stress drop (note that we are not relating here to the spontaneous stress drops that occur during stick slip events). A significant implication of this result is that the residual shear strength as obtained in PDC mode is **higher** than the residual shear strength obtained in BDC mode.

We note that in PDC mode the rougher surface exhibits slightly lower friction apparently due to asperity damage that took place in the sample. It is possible that at this level of normal stress the geometrical contribution of asperities<sup>22</sup> decreases and consequently higher roughness may not necessarily result in higher friction, as has also been observed by others.<sup>11,23,24</sup>

The peak shear stresses reached in every test are listed in Table 1 where it can be appreciated that they are largely similar for the two control modes.

The shear  $k_0$  [ $\frac{MPa}{mm}$ ] and normal  $k_n$  [ $\frac{MPa}{mm}$ ] stiffness values for the tested interfaces as obtained from the first shear and first normal loading segments, respectively, appear to be similar for the tested surfaces, irrespective of the control mode.

#### 3.2. Stick slip oscillations

Stick-slip oscillations are observed in both control modes, and they become more pronounced once ultimate shear stress is reached, although some stick-slip instabilities are detected during the initial shear

**Table 1**

Concentrated results of direct shear tests performed in both control modes. The shear stiffness measurement for sample Gb\_22 was not reliable because of the relatively high level of shear stress that was developed in the system during the initial normal loading segment, during which the horizontal position of the interface was maintained at zero using servo-control.

Sample ID	Initial RMS [ $\mu\text{m}$ ]	Test Type	Shear stiffness [ $\text{MPa}/\text{mm}$ ]	Normal stiffness [ $\text{MPa}/\text{mm}$ ]	Peak shear stress
Gb_1	525	BDC	14.96	11.97	4.14
Gb_21	565	PDC	12.18	8.51	4.26
Gb_2	6.9	BDC	7.5	9.16	3.79
Gb_22	6.8	PDC	–	9.08	4.56

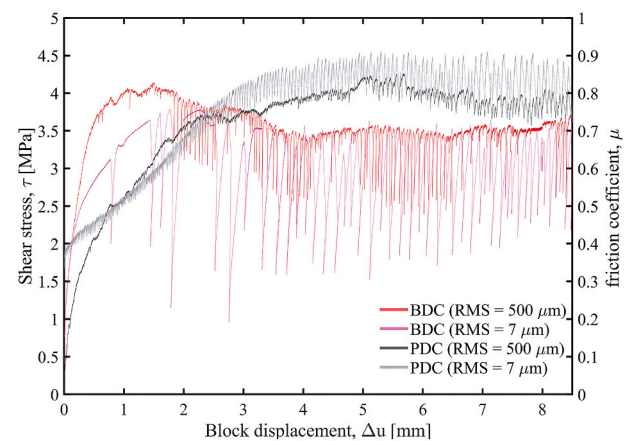


**Fig. 8.** Comparison between results obtained with BDC (reddish colors) vs. PDC (grey shades) modes for the fractured (RMS = 500  $\mu\text{m}$ ) and saw-cut (RMS = 7  $\mu\text{m}$ ) surfaces. (For interpretation of the references to color in this figure legend, the reader is referred to the Web version of this article.)

loading phase. Note that the average amplitude of the stick slip oscillations is much greater in the BDC mode, due to the attempt of the piston to correct for the spontaneous accelerations of the block in the slip cycles so that the actual block displacement rate obeys the prescribed rate, as explained in the Methods section above. The characteristics of the stick slip oscillations are further elaborated in the Discussion section.

As can be inferred from inspection of Fig. 8 classic steady state sliding is never achieved in our tests, rather stick slip oscillations of variable amplitudes are observed at the post peak region. To distinguish between real stick slips and electronic noise, stick slip instabilities are defined here when the spontaneous change from maximum to minimum shear stress within a single stick slip cycle is at least one order of magnitude higher than the force measurement resolution of the shear load cell (100 N or ca. 0.01 MPa).

The stress drops measured during stick slip cycles are plotted in Fig. 9, for both roughness levels as obtained with BDC (red) and PDC (black) modes. The solid grey lines represent our threshold shear force resolution. Both interfaces exhibit significant stress drops and the difference between the control modes is very apparent, with stick slip

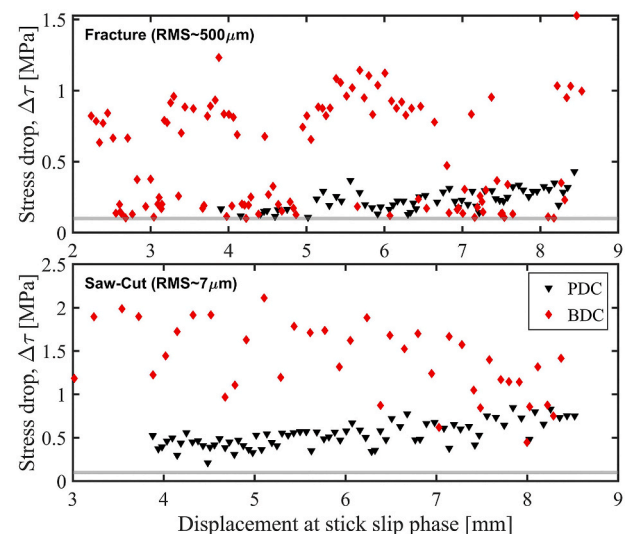


**Fig. 9.** Comparison between BDC (red) and PDC (black) stress drops for similar degree of roughness. The grey line represents the threshold value to count an instability event determined by loadcell resolution. (For interpretation of the references to color in this figure legend, the reader is referred to the Web version of this article.)

amplitude in BDC mode about twice as high as in the PDC mode: The average value of stress drops for the fractured surface in BDC is 0.53 MPa whereas for PDC is 0.23 MPa. The average stress drop in the saw-cut surface is 1.4 MPa in BDC mode, whereas in PDC mode the average stress drop is 0.53 MPa.

### 3.3. Slip rate effect

The shear response in both control modes is drastically affected by the imposed rate of the displacement in both control modes. To demonstrate the rate effect, we present in Fig. 10 velocity stepping results obtained for a polished sample (RMS = 5  $\mu\text{m}$ ). At a relatively fast shear rate of 0.1 mm/s stick slip oscillations are absent in both control modes (see Fig. 10a). Stick slips are prompted once the velocity is reduced by one order of magnitude to 0.01 mm/s which is the reference velocity in our broader experimental setup (see Fig. 10b). Note the great difference in stick slip amplitude between the control modes at this velocity; even though the “steady state” friction value in PDC is higher than in BDC mode, the amplitude of the oscillations is three time higher in BDC mode. The same behaviour is observed for sliding velocities of 0.05 mm/s (Figs. 10c) and 0.005 mm/s (Fig. 10d).

Sliding at 0.05 mm/s (Fig. 10c) is particularly interesting because in PDC mode sliding at this velocity is “semi-stable” whereas in BDC mode oscillatory stick slip behaviour is obtained. We may conclude therefore that the control modes modify, in addition to the amplitude of the stress drop instabilities, also the transition velocity from stale to non-stable sliding.

## 4. Discussion

A typical output of the electronic measurement transducers during stick slip instabilities is shown in Fig. 11 in detail, for an imposed shear displacement rate of 0.01 mm/s. The relative displacement of the block as obtained from the horizontal LVDT's ( $Y_{av}$ ) output in PDC mode is shown in black solid line (labeled PDC  $Y_{av}$  in Fig. 11) and the displacement of the shear piston as obtained from the piston transducer ( $S_y$ ) in this control mode is shown in black dashed line (labeled PDC  $S_y$  in Fig. 11). It can be seen that in PDC mode the motion of the block is arrested almost completely during “stick” phases while the motion of the piston continues to increase as per the prescribed piston displacement rate. This leads to an accumulation of elastic strain energy across the interface during “stick” phases which is released spontaneously during “slip” phases, as can be inferred from the obtained steps in the block displacement vs. time curve.

The behaviour of the system in BDC mode is very different. The motion of the piston is shown in dashed red line (labeled BDC  $S_y$  in

Fig. 11), and the motion of the block is shown in solid red line (labeled BDC  $Y_{av}$  in Fig. 11). Recall that in this mode the servo control feedback signal comes from the sliding interface using the average output from the two horizontal LVDT transducers that are located very close to the block. Therefore, the applied piston force and displacement rate are constantly adjusted by the servo control system so as to ensure that the block displacement conforms to the prescribed rate of 0.01 mm/s in our case. This has two important consequences: 1) It is not possible to obtain a real “stick” phase in this control mode, because the servo control system ensures that the motion of the block always adheres to the prescribed block displacement rate; this can be appreciated by comparing  $Y_{av}$  outputs in PDC and BDC modes in Fig. 11. It is readily apparent that during “stick” phases the motion of the block is continuous in BDC mode whereas in PDC mode the block motion is almost completely arrested. Consider Fig. 11b where the behaviour of the system is shown in greater detail, the velocity of the block during a “stick” phase is four times higher in BDC than in PDC mode; 2) Some elastic strain energy is inevitably being stored during the pseudo static “stick” phases in the BDC mode and is released spontaneously during the “slip” phases in this mode, as can be inferred from the spikes in the block displacement curve. The consequent forward accelerations of the block in BDC mode during the “slip” phases violate the prescribed block displacement rate, and therefore the servo control aims to correct this by pulling the loading piston backward, as is readily apparent from inspection of the dashed red line labelled BDC  $S_y$  in Fig. 11a. A single stick slip phase is shown in Fig. 11b where it can be seen that while the block slides rapidly forward for 0.01 mm in BDC mode the piston is actually being retracted by as much as 0.04 mm at the very same time. This decoupling between the block and the piston motion direction is made possible because of the release of the stored elastic energy in the machine components between the loading piston and the sliding block, namely the stiffness of the shear machine.

The automatic servo-controlled correction of the piston motion under BDC mode leads to artificially high stress drop amplitudes during stick slip cycles, as mentioned previously in this paper. This effect is illustrated in Fig. 12 which displays results from the stick slip oscillation phase of tests conducted under a prescribed shear displacement rate of 0.005 mm/s.

In addition to the artificially higher stress drop amplitudes during slip phases in BDC mode, it is readily apparent from inspection of Fig. 12a that the frequency of the stick slip events in BDC mode is higher than in PDC mode: 66.6 stick slip cycles per mm in BDC mode vs. 43.3 stick slip cycles per mm in PDC mode. Considering the classic spring – rider model of Jaeger et al.,<sup>19</sup> the frequency of the events should decrease when stress drop increases, if only the spring stiffness and the transition from static to dynamic friction coefficients determine the

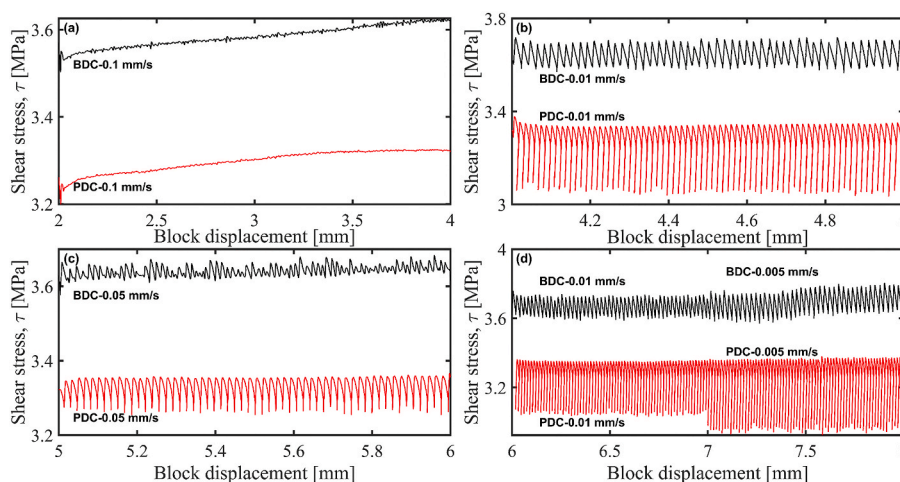


**Fig. 10.** Results of shear stress vs. relative displacement ( $Y_{av}$ ) for variable slip rates at the steady state stage of the experiments in BDC (red) and PDC (black) modes. a) stable sliding in both control modes for a 2 mm sliding distance with slip rate of 0.1 mm/s b) sliding distance of 1 mm with slip rate of 0.01 mm/s c) sliding distance of 1 mm with slip rate of 0.05 mm/s d) sliding distance of 2 mm with slip rate changed from 0.01 to 0.005 mm/s at 7 mm displacement. (For interpretation of the references to color in this figure legend, the reader is referred to the Web version of this article.)

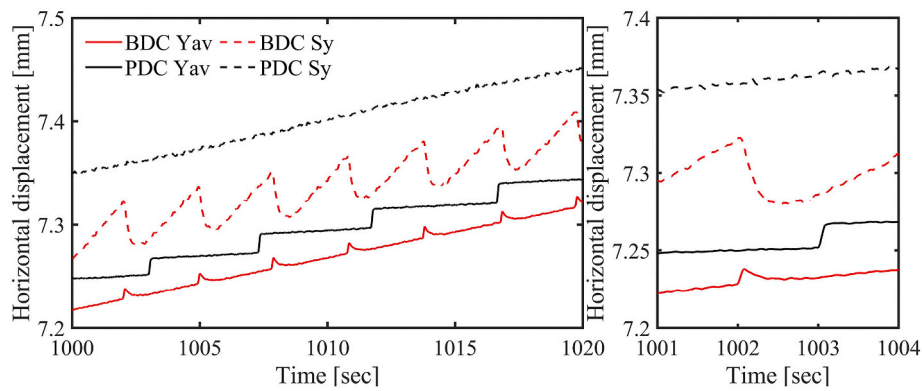


**Fig. 11.** Different behaviour during stick slip instabilities in BDC (red) and PDC (black) modes. The motion of the block is delineated in dashed lines (labelled  $Y_{av}$ ), and the motion of the piston in solid line (labelled  $S_y$ ). A) Output from several consequent stick-slip events, B) detailed plot of a single stick-slip event. (For interpretation of the references to color in this figure legend, the reader is referred to the Web version of this article.)

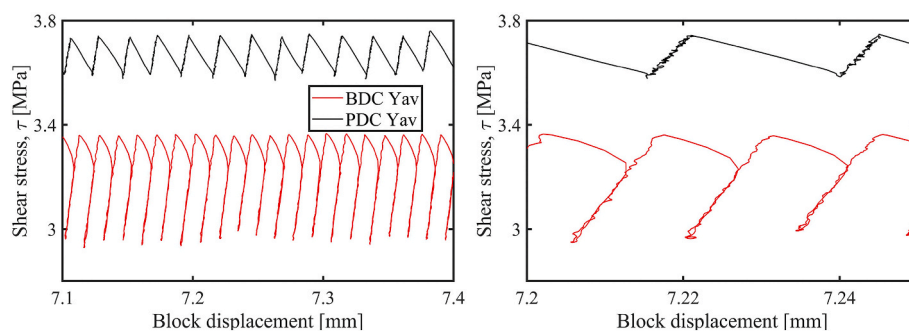


**Fig. 12.** Different stick slip frequencies in BDC (red) and PDC (black) modes for tests conducted at slip velocity of 0.005 mm/s on 5  $\mu$ m RMS surfaces. A) a sequence of consecutive stick-slip cycles, B) a detailed view illustrating that the retraction of the piston in BDC mode apparently increases the event frequency in BDC mode even though the stress drop magnitude is higher. (For interpretation of the references to color in this figure legend, the reader is referred to the Web version of this article.)

system response. But as can be seen in Fig. 12b, the automatic retraction of the loading piston in BDC mode interferes with the natural behaviour of the system and artificially reduces the amount of net forward block displacement during slip cycles, thus leading to the apparent higher event frequency in BDC mode when the stress drop is higher.

We have shown here, in some detail, that the imposed boundary conditions during direct shear testing of rock discontinuities have dramatic effects on the results. In stable sliding conditions that peak and residual shear strength may be different, and in case of stick slip instabilities, both the amplitude and frequency of the stick slip events will be determined by the control mode. We propose here that the selected boundary conditions in laboratory direct shear experiments should conform to the physical world application. If the stability of a single block resting on a plane of weakness in a rock mass is of interest, then it would be correct to conduct laboratory direct shear tests in BDC mode as the load on the block is derived primarily from its self-weight. The normal load control mode can be varied depending on the conditions in the field as discussed by Goodman.<sup>25</sup> If a single block on an inclined plane is considered then a constant normal stress boundary condition could be used in addition to the BDC mode. If however the stability of a block in a tunnel wall is considered, then a constant normal position boundary condition could be applied, in addition to the BDC mode. The PDC mode appears to be more appropriate for simulating the behaviour of crustal blocks moving across geological faults that are loaded by remote, far-field, tectonic stresses as well as massive landslides, allowing significant amount of elastic deformation in the rock mass that is coupled with shear sliding across the interface. Stick slip oscillations, which have been suggested by many authors as a plausible model for earthquakes (see Ref. 5,16,17,26,27) are much more relevant in that

case and indeed are modeled much more accurately in PDC mode.

## 5. Summary and conclusions

We compare here between two displacement control modes in close-loop servo-control direct shear experiments of rock discontinuities: Block Displacement Control (BDC) and Piston Displacement Control (PDC) modes. All tests are performed under an imposed constant normal stress of 5 MPa. Two levels of initial roughness in Gabbro interfaces are tested in both control modes. We find that in BDC mode the classic peak and residual shear strength behaviour is obtained, whereas in PDC mode the interfaces continuously exhibit shear displacement hardening. This leads to the interesting and important observation that in PDC mode the residual (or “steady-state”) shear strength is higher than in BDC mode.

Beyond the significance of the results to experimental investigations of shear strength of rock interfaces, we find that sliding instabilities manifest very differently between the two control modes. Results obtained with PDC mode match theoretical expectations considering the classical spring – rider model. Results obtained with the BDC mode during stick slip instabilities are in fact wrong because of the tendency of the servo control system to keep moving the block forward during “stick” cycles and then to pull it backward during “slip” cycles. This manifests in artificially higher stress drops during stick slip events and higher stick slip event frequency when testing sliding instabilities in BDC mode.

We suggest that testing rock discontinuities in BDC mode would be more appropriate for rock engineering purposes when the stability of single blocks loaded primarily by their self-weight is of interest. Testing rock discontinuities in PDC mode would be more accurate for

seismological purposes focusing on sliding instabilities, as both the stress drop and event frequency would be modeled much more accurately in the lab using the PDC mode.

#### Declaration of competing interest

The authors declare that they have no known competing financial interests or personal relationships that could have appeared to influence the work reported in this paper.

#### Acknowledgements

This research is funded by Israel Science Foundation, contract no. 937/17. Bob Griffin formerly of TerraTek Inc. is thanked for assistance with the technical drawing of the shear frame. Liran Goren and Yuval Tal of BGU are thanked for stimulating discussions on stick slip instabilities.

#### References

- Muralha J, Grasselli G, Tatone B, Blümel M, Chryssanthakis P, Yuqing J. ISRM suggested method for laboratory determination of the shear strength of rock joints: revised version. *Rock Mech Rock Eng.* 2014;47:291–302.
- Fitzsimons SJ, McManus KJ, Sirota P, Lorrain RD. Direct shear tests of materials from a cold glacier: implications for landform development. *Quat Int.* 2001;86:129–137.
- Sinnathamby G, Korkiala-Tanttu L, Forés JG. Interface shear behaviour of tunnel backfill materials in a deep-rock nuclear waste repository in Finland. *Soils Found.* 2014;54:777–788.
- Towhata I, Yamazaki H, Kanatani M, Lin C, Oyama T. Laboratory shear tests of rock specimens collected from site of Tsao-ling earthquake-induced landslide. *Tamkang J Sci Eng.* 2001;4:209–220.
- Dieterich JH. Time-dependent friction and the mechanics of stick-slip. In: *Anonymous Rock Friction and Earthquake Prediction*. Springer; 1978:790–806.
- Dieterich JH. Modeling of rock friction: 1. Experimental results and constitutive equations. *J Geophys Res: Solid Earth.* 1979;84:2161–2168.
- Karner SL, Marone C. Effects of loading rate and normal stress on stress drop and stick-slip recurrence interval. In: *Geophysical Monograph-American Geophysical Union*. 120. 2000:187–198.
- Leeman J, Scuderi MM, Marone C, Saffer D. Stiffness evolution of granular layers and the origin of repetitive, slow, stick-slip frictional sliding. *Granul Matter.* 2015;17:447–457.
- Mclasky GC, Yamashita F. Slow and fast ruptures on a laboratory fault controlled by loading characteristics. *J Geophys Res: Solid Earth.* 2017;122:3719–3738.
- Ruina A. Slip instability and state variable friction laws. *J Geophys Res: Solid Earth.* 1983;88:10359–10370.
- Biegel RL, Wang W, Scholz CH, Boitnott GN, Yoshioka N. Micromechanics of rock friction I. Effects of surface roughness on initial friction and slip hardening in westerly granite. *J Geophys Res: Solid Earth.* 1992;97:8951–8964.
- Tsesarsky M, Talesnick ML. Mechanical response of a jointed rock beam—numerical study of centrifuge models. *Int J Numer Anal Methods GeoMech.* 2007;31:977–1006.
- Kilgore B, Beeler NM, Lozos J, Oglesby D. Rock friction under variable normal stress. *J Geophys Res: Solid Earth.* 2017;122:7042–7075.
- Morad D, Hatzor YH, Sagy A. Rate effects on shear deformation of rough limestone discontinuities. *Rock Mech Rock Eng.* 2019;52:1613–1622.
- Rabinowicz E. The intrinsic variables affecting the stick-slip process. *Proc Phys Soc.* 1958;71:668.
- Brace WF, Byerlee JD. Stick-slip as a mechanism for earthquakes. *Science.* 1966;153:990–992.
- Byerlee JD, Brace WF. Stick slip, stable sliding, and earthquakes—effect of rock type, pressure, strain rate, and stiffness. *J Geophys Res.* 1968;73:6031–6037.
- Ruina AL. *Friction Laws and Instabilities: A Quasi-Static Analysis of Some Dry Friction Behaviour*. Ph.D.thesis. Division of Engineering, Brown University; 1980.
- Jaeger JC, Cook NG, Zimmerman R. *Fundamentals of Rock Mechanics*. John Wiley & Sons; 2009.
- Hudson JA, Crouch SL, Fairhurst C. Soft, stiff and servo-controlled testing machines: a review with reference to rock failure. *Eng Geol.* 1972;6:155–189.
- Badt N, Hatzor YH, Toussaint R, Sagy A. Geometrical evolution of interlocked rough slip surfaces: the role of normal stress. *Earth Planet Sci Lett.* 2016;443:153–161.
- Ladanyi B, Archambault G. Evaluation de la resistance au cisaillement d'un massif rocheux fragmente. In: *Proc.24th Intl.Geol.Cong.* 1972:249–260.
- Marone C, Cox S. Scaling of rock friction constitutive parameters: the effects of surface roughness and cumulative offset on friction of gabbro. *Pure Appl Geophys.* 1994;143:359–385.
- Ohnaka M. Experimental studies of stick-slip and their application to the earthquake source mechanism. *J Phys Earth.* 1973;21:285–303.
- Goodman RE. *Introduction to Rock Mechanics*. New York: Wiley; 1989.
- Leeman JR, Saffer DM, Scuderi MM, Marone C. Laboratory observations of slow earthquakes and the spectrum of tectonic fault slip modes. *Nat Commun.* 2016;7:1–6.
- Marone C. Laboratory-derived friction laws and their application to seismic faulting. *Annu Rev Earth Planet Sci.* 1998;26:643–696.